Available online at www.sciencedirect.com
SCIENCE DIRECT®
Optical Materials 23 (2003) 513–518
OPTICAL Materials
www.elsevier.com/locate/optmat

Photoluminescence characteristics of Ti_2S_3 nanoparticles embedded in sol–gel derived silica xerogel

Ping Yang [a], Mengkai Lü [a,*], Chunfeng Song [a], Suwen Liu [a], Zi Ping Ai [b], Guangjun Zhou [c], Dong Xu [a], Duorong Yuan [a], Xiufeng Cheng [a]

[a] State Key Laboratory of Crystal Materials, Shandong University, Jinan 250100, PR China
[b] The Experimental Center of Shandong University, Jinan 250100, PR China
[c] Shandong Supervision and Inspection Institute for Product Quality, Jinan 250100, PR China

Received 2 July 2002; received in revised form 3 December 2002; accepted 7 January 2003

Abstract

Ti_2S_3 nanocrystallites embedded in sol–gel derived silica xerogel have been prepared. Their photoluminescence (PL) characteristics have been evaluated and compared with those of pure silica xerogel. UV–vis absorption spectra, transmission electron micrograph, excitation spectra and PL spectra of the doped and undoped samples have all been investigated. Two emission peaks have been observed from the doped samples, one at 440 nm ($\lambda_{ex} = 380$ nm) while the other at 600 nm ($\lambda_{ex} = 550$ nm). The latter has been assigned to the Ti_2S_3 nanocrystallites in the silica xerogel. Therefore, a novel luminescence property can be observed by introducing the semiconductor nanoparticles into the silica xerogel.

Keywords: Silica xerogel; Nanocrystals; Luminescence; Sol–gel

1. Introduction

Semiconductor nanoparticles embedded in organic polymer and inorganic matrices have two important aspects. The first involves that isolation and stabilization of small clusters through surface passivation in a solid phase matrix [1]. The unique electronic and optical properties (quantum effects in nanostructures) are presented enough [2,3]. The second, the direct applications of nanometer scales materials are difficult. If the nanoparticles are embedded in the supporting media, the semiconductor nanocrystallites can be used widely. These embedded structures have some advantages and offer attractive options: for example, the chemical and mechanical stabilities, the decrease of the total capacitance to optical waveguides and photonic devices [4,5]. Because the structure of the sol–gel derived oxide networks are strongly affected by the concentration of the interacting species, their ratios, the reaction medium and so on, the nanoparticles can affected the PL characteristics of the sol–gel derived silica xerogel. In addition, the matrices maybe affect the PL properties of semiconductor nanoparticles. Therefore,

* Corresponding author. Tel.: +86-531-8564591; fax: +86-531-8565403.
E-mail address: pyangxx@163.com (M. Lü).

0925-3467/03/$ - see front matter © 2003 Elsevier B.V. All rights reserved.
doi:10.1016/S0925-3467(03)00005-3

semiconductor nanocrystallites embedded in silica glasses have received much attention due to people's fundamental interest in the quantum confinement effect and potential applications for nonlinear optical devices [6–10].

Sol–gel SiO_2 glass is becoming increasingly important in modern display and lighting technology. Also, silica xerogels have many novel physical properties that make them serve as the matrix materials for nanocomposite. Many optical studies have been reported for Ti, V, Cr, Mn, Fe, Co, Ni and Cu impurities in II–VI, III–V and I–III–VI_2 semiconductors [11,12]. The spectra exhibit weak, sharp absorption features below the fundamental absorption edges and has been interpreted as the intra-atomic d–d transitions within the d^n multiplet of the impurity ions [12,18].

In this paper, we present the results of the study on the PL properties of Ti_2S_3 nanoparticles embedded in silica xerogel by sol–gel processing for the first time. The Ti_2S_3 nanoparticles are well-distributed in the xerogel matrices. Two stable emission bands have been observed from Ti_2S_3 nanoparticles embedded in sol–gel silica xerogel. The Ti_2S_3 nanoparticles have a sharp emission band in porous silica xerogel.

2. Experimental

Silica sols were prepared by sol–gel process using tetra-ethylorthosilicate (TEOS, $Si(OC_2H_5)_4$). The $Si(OC_2H_5)_4$ was first hydrolyzed and stirred for 1 h. The volume ratio of water:TEOS:ethanol:HCl (6 N) is 1:1:0.5:0.00125 (the mole ratio of water:TEOS:ethanol is ~12.42:1:1.92). Then, HCl in the sol was neutralized with a base for obtaining stable Ti_2S_3 nanoparticles in the silica xerogel. NH_4OH solution (0.1 N, the addition of NH_4OH was the same as that of HCl in the sol) was added in the resultant homogeneous sol and stirred for about 20 min. After that, $TiCl_3$ (the color of Ti^{3+} solution is purple) and Na_2S solutions were added in the resultant homogeneous sol and stirred for 30 min. Because Ti^{3+} ions are unstable in aqueous medium and turn to Ti^{4+} ions, the sol–gel reactive process was in weakly reductive condition to control the oxygenation of Ti^{3+} ions. The mole ratio of Ti^{3+} and S^{2-} ions in the silica xerogel is 2:3. The mole ratios of Ti_2S_3 in the silica xerogel are 0.045, 0.090, 0.134, 0.224 and 0.500%, respectively. The sol was kept at room temperature until its complete gelation in a vacuum dryer. Final drying of the gel was obtained after one week at room temperature. The xerogel was then heated in a weakly reductive atmosphere at a rate of 6 °C/h up to the temperature of 50 °C, and kept 10 h at this temperature.

The absorption spectra of the samples were measured using a Hitachi U-3500 spectrophotometer. The fluorescent spectra of the samples were measured by a Hitachi M-850 fluorescence spectrophotometer. Particle core size was measured with a JEM-100CX II transmission electron microscope (TEM) at 100 kV. Selected area electron diffraction was also carried out on the TEM chamber. The samples were prepared by casting a drop of the sol of the sample on to a 300-mesh copper grid.

3. Results and discussion

Because the aggregation of the Ti_2S_3 nanoparticles, the size of the Ti_2S_3 nanoparticles increases with increasing the mole ratios of Ti_2S_3 in the silica xerogel. Thus, the transparence of the samples doped with Ti_2S_3 nanoparticles decreases with increasing the mole ratios of Ti_2S_3 in the silica xerogel. When the mole ratio of Ti_2S_3 in the silica xerogel is $<0.269\%$, the doped sample is transparence. When the mole ratio of Ti_2S_3 is 0.269%, the doped sample is translucence and the sol of the doped sample was transited into gel after about 5 h at room temperature.

Fig. 1 shows the absorption spectra of the doped and undoped samples. Fig. 1 indicates that the absorption spectra of the doped sample have a red shift with increasing the impurity mole ratios of Ti_2S_3. The absorption shoulder peak and band edge of the doped sample are different from those of the undoped sample. The absorption spectrum of the luminescent materials is related to their band gap. By introducing the nanoparticles into silica xerogel, the band gap of the nanocomposite of Ti_2S_3 and silica xerogel is different from that of

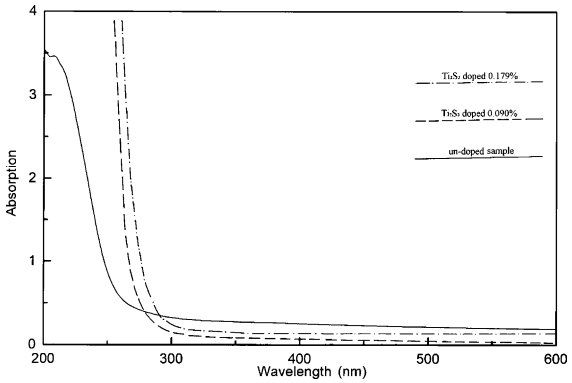

Fig. 1. Absorption spectra of doped and undoped samples (mean impurity mole ratio).

the undoped silica xerogel. The nanocomposite can absorb the photons with different energy as compared with the undoped silica xerogel. Therefore, the absorption spectra of the doped samples are significantly different from those of pure silica xerogel.

TEM observations of the silica xerogel sample doped with Ti_2S_3 nanoparticles are shown in Fig. 2. The mole ratios of Ti_2S_3 in *a*, *b* and *c* silica xerogel samples are 0.134%, 0.224% and 0.5%, respectively. The dark particles in TEM micrograph are Ti_2S_3 nanoparticles. Because the doped sample has only a crystal phase (Ti_2S_3) and silica phase exhibits a non-crystalline structure, the nanoparticles are identified as Ti_2S_3 nanocrystallites. The particle size of Ti_2S_3 nanocrystallites increases with increasing the impurity ratio of Ti_2S_3. Also, Fig. 2 shows a selected area electron diffraction pattern of the doped sample (in Fig. 2d–f are the electron diffraction pattern of a, b and c, respectively). The crystallinity of the particles increases with the increasing of the ratios of Ti_2S_3.

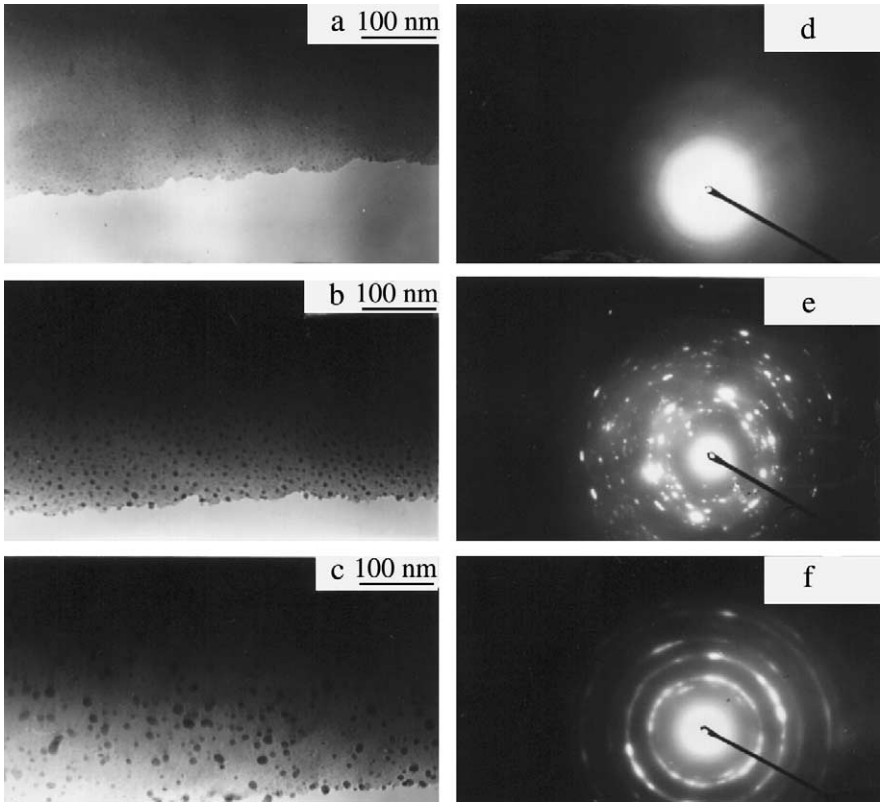

Fig. 2. (a), (b) and (c) Transmission electron micrograph of the doped samples; (d), (e) and (f) electron diffraction pattern of the doped samples.

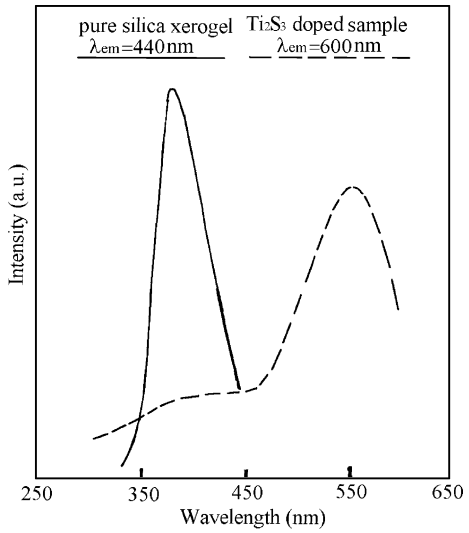

Fig. 3. Excitation spectra of the doped and undoped samples.

The excitation spectra of doped and undoped samples are shown in Fig. 3. The excitation spectrum of Ti_2S_3 nanoparticles embedded in the silica xerogel consists of two peaks, one at 380 nm ($\lambda_{em} = 440$ nm) and the other at 550 nm ($\lambda_{em} = 600$ nm). The excitation spectrum of the pure sol–gel silica xerogel has only one excitation peak (380 nm, $\lambda_{em} = 440$ nm). Therefore, we think that the second excitation peak of the doped samples is associated with the Ti_2S_3 nanoparticles in the sol–gel silica xerogel.

Fig. 4 shows the emission spectra of the pure and doped samples. The emission peak of the undoped sample is at 440 nm. The PL spectrum of Ti_2S_3 nanoparticles embedded in sol–gel silica xerogel consists of two emission peaks, one at 440 nm ($\lambda_{ex} = 380$ nm) and the other at 600 nm ($\lambda_{ex} = 550$ nm). When excitation wavelength is 380 nm, the emission peak of 600 nm is very weak. The relative PL intensity of the doped samples increases dramatically as comparing with that of the pure sample (when the doped mole ratio of Ti_2S_3 nanoparticles is 0.090%, the relative PL intensity of the doped sample is about four times of that of the undoped sample). Thus, the second emission peak (600 nm) and excitation peak (550 nm) of the doped samples are assigned to the Ti_2S_3 nanoparticles in the sol–gel silica xerogel. The PL intensities of the doped samples increase remarkably as comparing with that of Ti^{3+}-doped ZnS nanocrystallites [12].

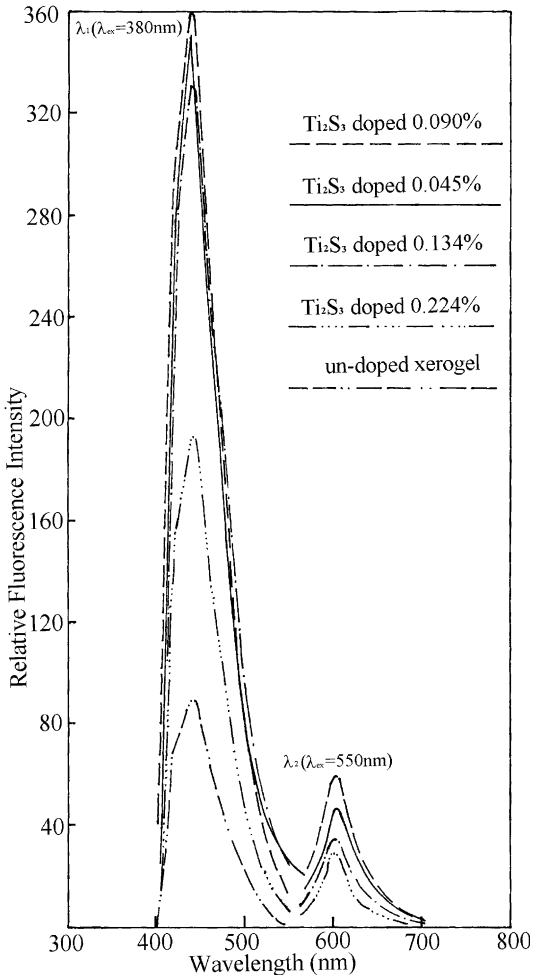

Fig. 4. Emission spectra of the doped and undoped samples (mean impurity mole ratio).

The origin of the luminescence in sol–gel derived silica gels is still not understood yet [13]. Three possible mechanisms, i.e., defect mechanism [14], charge transfer mechanism [15] and carbon impurity mechanism [16], are proposed to explain the luminescent phenomena in sol–gel derived silica gels. According to the defect mechanism, different network structures will produce different defects during the drying process, and will further produce different luminescence centers and lumi-

nescence properties in the silica xerogels [13]. For example, the Si dangling bond and oxygen vacancy (E' center) is assumed to be the luminescence species for strong blue emission of the sol–gel porous silica glass [17]. Because Ti_2S_3 nanoparticles can lead to the increase of the disorder of silica network in the forming processes, the concentration of the luminescent defects increases with the introducing of Ti_2S_3 nanoparticles into the silica xerogel. Thus, the PL intensity of the doped sample dramatically increases.

By comparing the luminescence of the pure xerogel sample with the Ti_2S_3 embedded in the sol–gel silica xerogel an emission band consisting of two contributions can be observed. The shorter wavelength contribution has a maximum at 440 nm, and is ascribed to the defect luminescence and Ti_2S_3 centers in the sol–gel silica xerogel. The second contribution is ascribed to the centers involving Ti_2S_3 nanoparticles (a maximum at 600 nm). Since the luminescence of titanium centers in the Ti_2S_3 nanocrystallites embedded in the sol–gel silica xerogel involves a transition from the conduction band to the ground state level of trivalent titanium, situated near the valence band, no concentration dependence on the spectral position can be observed. But, the PL intensities of the doped samples vary with increasing the ratio of Ti_2S_3 nanocrystallites in the silica xerogel because of the concentration quenching effect.

The band gap of semiconductor nanocrystallites E'_g as a function of particles radius is given by [18]: $E'_g = [E_g^2 + 2\hbar^2 E_g(\pi/r)^2/m^*]^{1/2}$, E_g: the band gap of the bulk semiconductor, $\hbar$: Planck's constant, m^* is the effective mass of electron, taking $m^* = 0.085m_e$, m_e: being the free electron mass [18]. By introducing Ti_2S_3 nanoparticles in the silica xerogel, one can expect luminescence from a different origin. The structure defects of the silica xerogel can be affected by the neighboring Ti_2S_3 nanoparticles, or the Ti_2S_3 nanoparticles can be active centers. Because of the surface passivation of silica xerogel on Ti_2S_3 nanoparticles, the size distribution of Ti_2S_3 nanoparticles embedded in the sol–gel silica xerogel is narrow as compared with pure Ti_2S_3 nanocrystallites. The luminescent monochromaticity of Ti_2S_3 nanoparticles embedded in the silica xerogel increases comparing with that of pure Ti_2S_3 nanocrystallites. Therefore, the sharp emission band of trivalence titanium has been observed from the Ti_2S_3 nanoparticles embedded in the sol–gel silica xerogel.

4. Conclusion

SiO_2 xerogel doped with Ti_2S_3 nanocrystals has been prepared by using sol–gel process. The PL characteristics of doped and undoped samples have all been investigated. By introducing Ti_2S_3 nanoparticles into the sol–gel silica xerogel, two PL peaks ($\lambda_{em1} = 440$ nm, $\lambda_{em2} = 600$ nm) have been observed. The novel emission peak is assigned to the Ti_2S_3 nanoparticle embedded in the porous silica xerogel. The sharp emission band of trivalent titanium has been observed from the doped samples. The novel emission phenomenon is very important for the applications and research of nanometer scale luminescence materials and the sol–gel silica xerogel.

Acknowledgements

The authors are grateful for the support of the Natural Science Foundation of China (grant no. 69890230).

References

[1] M.A. Olshavsky, H.R. Allcock, Chem. Mater. 9 (1997) 1367.
[2] C.B. Murray, D.J. Norris, M.G. Bawendi, J. Am. Chem. Soc. 115 (1993) 8706.
[3] C.B. Murray, C.R. Kagan, M.G. Bawendi, Science 270 (1995) 1335.
[4] J.A. Conklin, L. Salvati, A. Sen, Chem. Mater. 2 (1990) 772.
[5] X. Li, J.R. Fryer, D.J. Cole-Hamilton, J. Chem. Soc., Chem. Commun. (1994) 1715.
[6] D. Nesheva, H. Hofemister, Solid State Commun. 114 (2000) 511.
[7] D. Nesheva, C. Raptis, Z. Levi, Z. Popovic, I. Hinic, J. Lumin. 82 (1999) 233.
[8] P. Maly, T.M. Shi, J. Lumin. 90 (2000) 129.
[9] T. Komatsu, T. Nakagawa, K. Matusita, J. Mater. Sci. Lett. 14 (1995) 1023.

[10] G. Tamulatitis, V. Gulbinas, G. Kodis, A. Dementjec, L.V. Unas, J. Appl. Phys. 88 (2000) 178.
[11] G.R. Olbright, N. Peyghambarian, Appl. Phys. Lett. 48 (1986) 1184.
[12] P. Yang, M. Lü, D. Xu, D. Yuan, C. Song, G. Zhou, Appl. Phys. A 74 (2002) 525.
[13] J. Lin, K. Baerner, Mater. Lett. 46 (2000) 86.
[14] B.E. Yoldas, J. Mater. Res. 5 (1990) 1157.
[15] J. Garcia, M.A. Mondragon, C. Tellez, S.A. Campero, V.M. Castano, Mater. Chem. Phys. 41 (1995) 15.
[16] W.H. Green, K.P. Le, J. Grey, T.T. Au, M.J. Sailor, Science 276 (1997) 1826.
[17] N. Chiodini, F. Meinardi, F. Morazzoni, A. Paleari, R. Scotti, D.D.A. Martino, Appl. Phys. Lett. 76 (2000) 209.
[18] M. Mukherjee, A. Datta, S.K. Pradhan, D. Chakravorty, J. Mater. Sci. Lett. 15 (1996) 654.